*Progress In Electromagnetics Research M, Vol. 43, 101–108, 2015*

# Design and Performance Index Comparison of the Permanent Magnet Linear Motor

**Fairul Azhar[1, *], Hiroyuki Wakiwaka[2], Kunihisa Tashiro[2], and Masami Nirei[3]**

**Abstract**—In this paper, a cylindrical permanent magnet linear motor (PMLM), which has a high performance, was designed and developed, because the motor has a zero normal force and a higher thrust density. The structure of the motor plays a vital role at the stage of design. During the design stage, several models of the PMLM that had different structural parameters were simulated using FEM software, and the model that produced the high-performance was identified. The structural parameters involved include the radius and height of the permanent magnet, $r_{pm}$ and $h_{pm}$, the height of coil, $h_c$, and the shaft radius, $r_s$, within a fixed total radius, $r_{total}$. To prove its high-performance characteristics, the performance of the PMLM was then compared to the commercialized PMLM using four performance indexes which are thrust $F$, thrust constant $k_f$, motor constant $k_m$ and motor constant square density $G$. About 200 commercialized PMLMs with three different types have been chosen which are the slot type PMLM, slotless type PMLM and shaft motor. Based on the comparisons, the designed PMLM had a better performance than the commercialized PMLM. In order to validate the simulation result, the PMLM was manufactured. The simulation and measurement static thrust characteristics were then compared, and it was found that the simulated thrust had a good agreement with the measured one.

## 1. INTRODUCTION

Generally, a linear motor is used to produce a direct linear motion. Compared to the traditional style of the linear motion system which is composed of a rotational motor attached with a motion translation such as belts, gears and ball screws, the linear motor is able to produce a linear motion directly without using any of the motion translations mentioned previously. The linear motor has several advantages such as a higher dynamic performance, a simpler structure, an improved reliability by reducing some parts and a higher efficiency due to the avoidance of the motion translation from rotary to linear motion [1–3]. However, the cost of the linear motor development is dependent on the stroke. The higher the stroke is, the higher the cost of development is [4, 5]. The linear motor can be divided into two types, which are the permanent magnet type and non-permanent type (i.e., switched reluctance linear motor and linear induction motor). However, due to the two sources of magnetic field that exist in the permanent magnet type of the linear motor, it is able to produce a higher thrust density than its counterpart.

The PMLM can be designed either in a rectangular/flat shape or a cylindrical/tubular shape [6]. However, in this paper, the cylindrical shape of the PMLM was chosen as opposed to the rectangular kind, based on several advantages that the former has. The cylindrical shape of the PMLM does not need end winding as the rectangular shape does. All coils in the cylindrical shape are active participants to the magnetic field and the thrust production [7]. This condition increases the coil efficiency and power to weight ratio. Furthermore, the cylindrical shape of the PMLM is composed of a ring shape of the coil

*Received 12 July 2015, Accepted 12 August 2015, Scheduled 18 August 2015*

* Corresponding author: Fairul Azhar bin Abdul Shukor (fairul.azhar@utem.edu.my).

[1] Faculty of Electrical Engineering, Universiti Teknikal Malaysia Melaka, Durian Tunggal, Melaka 76100, Malaysia. [2] Faculty of Engineering, Shinshu University, Nagano 380-8553, Japan. [3] National Institute of Technology, Nagano College, 716, Tokuma, Nagano 381-8550, Japan.

winding. The ring shape coil winding is easy to manufacture and suitable to be industrially produced. The cylindrical shape of the PMLM also has the features of self-neutralization of the normal force [8] and reduces the support mechanism requirement [9]. On top of that, the cylindrical shape of the PMLM has a compact structure and high force density [9–11]. However, the cylindrical shape of the PMLM limits the maximum stroke. Exceeding the limit stroke may cause vibrations and mechanical damage to the PMLM [8].

In this paper, the PMLM is designed to have a high-performance characteristic. Generally, the performance of the PMLM is evaluated using thrust. However, the thrust of the PMLM is proportional to current $I$, input power $P$ and volume $v$ [12]. Therefore, instead of just thrust, the performance of the PMLM will also be evaluated using other performance indexes which are thrust constant $k_f$, motor constant $k_m$, and motor constant square density $G$. As a benchmark, the performance index of the PMLM has been compared to the commercialized PMLM. Three types of PMLMs have been chosen for the comparisons which are the slot type, the slotless type and the shaft motor.

## 2. PERFORMANCE INDEX OF THE PMLM

During design and development of the PMLM, most of the researchers will use thrust as an evaluation factor. However, the thrust $F$ is influenced by other factors such as current $I$, input power $P$, and volume $v$. Figure 1 shows an example of the PMLM structure where a box labeled as $a_{thrust}$ is an area where thrust is developed. As well known, the volume $v$ is the determination factor of the PMLM performance. The higher the volume $v$ is, the higher thrust could be produced. It is due to bigger area of $a_{thrust}$ and size of coil of the PMLM on higher volume $v$ of the PMLM, hence higher current $I$ and input power $P$ could be injected. Therefore, in order to make a valid comparison between PMLMs, despite of only depending on the thrust, another performance index should be used. Several researchers suggest to use a motor constant square density $G$ as one of the performance indexes [13–16]. In the motor constant square density $G$, the factors of volume $v$ and input power $P$ will be normalized and make performance comparison between PMLMs with different volumes $v$ and input powers $P$ valid. On top of that, the other performance indexes such as thrust constant $k_f$ and motor constant $k_m$ could also be used as the performance indexes as being used in [17, 18]. For the thrust constant $k_f$, current $I$, excited during thrust production will be normalized while for the motor constant $k_m$, input power $P$ injected during thrust production will be normalized. Even though in other references such as in [18, 19], the thrust density in unit of (N/cm$^3$) was suggested to be implemented during performance evaluation; however, by using motor constant, square density is more comprehensive since it also takes into account of normalizing the input power $P$.

The PMLM's performance was evaluated using four performance indexes. The performance indexes are thrust $F$, thrust constant $k_f$, motor constant $k_m$, and motor constant square density $G$. The performance indexes were calculated using a series of equations below,

$$k_f = \frac{F_{ave}}{I} \quad (\mathrm{N/A}) \tag{1}$$

$$k_m = \frac{F_{ave}}{\sqrt{P}} \quad (\mathrm{N}/\sqrt{\mathrm{W}}) \tag{2}$$

$$G = \frac{F_{ave}^2}{Pv} \quad (\mathrm{N^2}/(\mathrm{Wm^3})) \tag{3}$$

where, $k_f$ is the thrust constant in (N/A), $F_{ave}$ the average thrust in (N), $I$ the current in each coil in (A), $k_m$ the motor constant in (N/$\sqrt{\mathrm{W}}$), $P$ the input power in (W), $G$ the motor constant square density in (N$^2$/(Wm$^3$)), and $v$ the motor volume in (m$^3$).

In order to make a valid comparison of the performance index especially for the motor constant square density $G$, the PMLM volume $v$ was calculated by only considering the area where thrust is developed for each type of PMLM as shown in the example in Figure 1. Figure 2 shows the comparison of the performance indexes between the commercialized PMLMs. It involves about 200 models from several motor manufacturers with three different types of PMLMs. As shown in Figure 2(a), the thrust $F$ of the PMLM is directly proportional to the volume $v$. Therefore, a comparison of the PMLM based only on the thrust $F$ is not adequate if volume of the PMLM, $v$, is not considered. On top of that, the

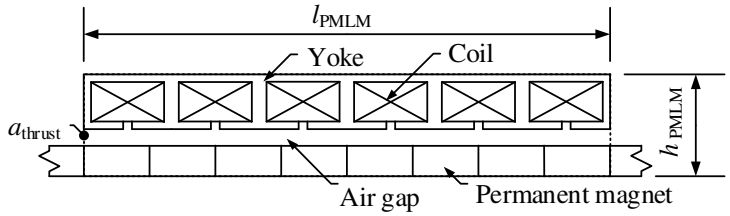


**Figure 1.** Example of PMLM structure.

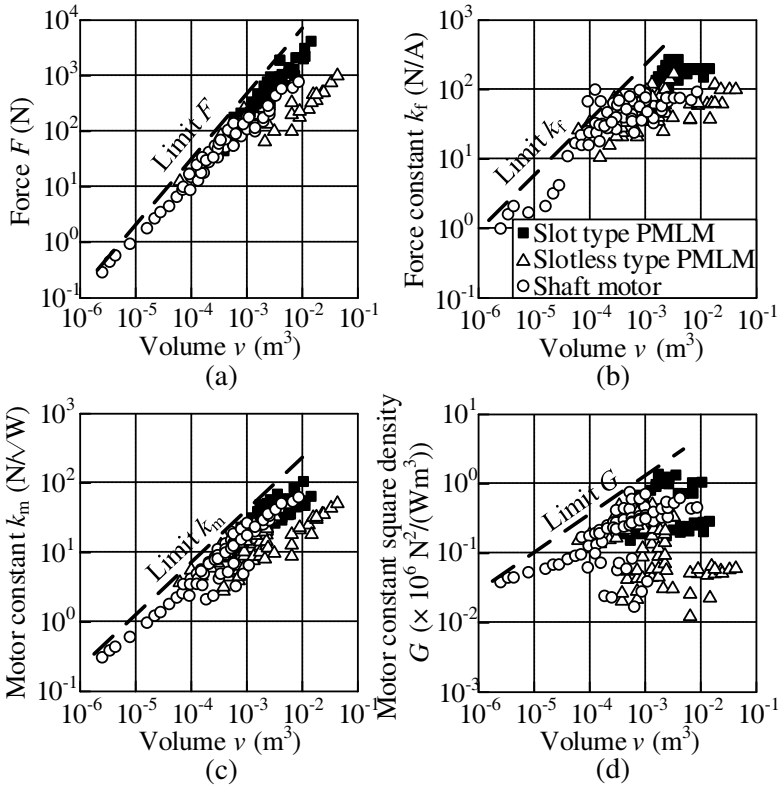


**Figure 2.** Comparison of performance index between commercialize PMLM. (a) Thrust, $F$. (b) Force constant, $k_f$. (c) Motor constant, $k_m$. (d) Motor constant square density, $G$.

thrust also depends on other parameters such as current $I$ and input power $P$. Therefore, in the same figure, the comparisons of the other performance indexes between the commercialized PMLMs are also presented. Parameters such as current $I$, input power $P$, and volume $v$ were normalized in comparison of the thrust constant $k_f$, motor constant $k_m$, and motor constant square density $G$. The comparison was done within a similar size of the PMLM. In this case, volume $v$ was chosen to represent the size of the PMLM. A comparison using volume $v$ is a more convenient way, especially for observing the limitation of the performance index of the PMLM.

Also shown in Figure 2, the existing commercialized PMLM has a limitation on all performance indexes. Even though the commercialized PMLM had been taken from several linear motor manufacturers, the performance index limitation shows a linear relationship to the volume $v$. Therefore, the aim of this paper is to design a PMLM that has a performance index higher than its limit. Several structure parameters were varied, and the best model was observed. The performance index of the best model of the PMLM was compared to the performance index of the commercialized PMLM. The results of the comparison will be discussed in the next sections.

## 3. DESIGN OF THE PMLM FOR A HIGHPERFORMANCE INDEX

Figure 3 shows the basic structure and structure parameters of the PMLM. It consists of a coil embedded inside a slotted stator yoke on the stator side and a Halbach magnetization direction arrangement of the permanent magnet on the mover side. During the design of the PMLM, while several structure parameters such as the coil pitch $\tau_c$ and PM pitch $\tau_{pm}$ were fixed, the other structure parameters, such as the radius of the permanent magnet, rpm, height of the permanent magnet $h_{pm}$, shaft radius $r_s$, and height of coil $h_c$, were varied within a possible range. Models of PMLM were simulated and compared to each other. The model of the PMLM which produced the highest thrust was acquired. During the design stage of the PMLM, a dynamic thrust will be observed. A balanced three-phase power supply was used to energize the PMLM's coil. This is done to represent a near actual operation and performance of the PMLM. Based on the dynamic thrust obtained, the average thrust $F_{ave}$ was calculated and used for the calculation of the PMLM's performance index.

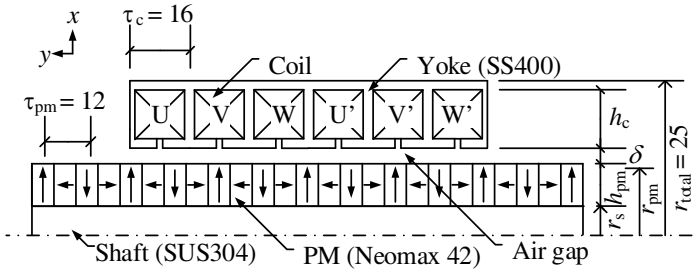


**Figure 3.** Basic structure and structure parameters of the PMLM (unit: mm).

The design process consisted of two stages. At the first stage, the shaft radius $r_s$ was set to 1 mm while the height of the permanent magnet $h_{pm}$ was varied from 1 mm to the highest possible value by considering the other structure parameters. Due to the fixed total radius $r_{total}$, an increment of the height of the permanent magnet $h_{pm}$ will reduce the height of the coil $h_c$ accordingly. Each model of the PMLM was simulated. The thrust characteristic at a full range of the mover displacement $x$ was observed, and the model of the PMLM that produced the highest thrust was identified. Due to variation of height of coil $h_c$, the coil turns $N$ of each model of PMCLSM will be varied too. It will also affect the resistance $R$ and current $I$ for each coil. The input power $P$ for each model has been fixed to 150 W for each phase. Based on the value of input power, coil turns, coil turns $N$, coil resistance $R$ and current $I$ were calculated using,

$$N = \frac{1}{\xi}\left(\frac{W_c}{\phi_C} \times \frac{h_c}{\phi_C}\right) \tag{4}$$

$$R = N^2\frac{\rho l}{a} = \frac{1}{\xi}\left(\frac{W_c}{\phi_C} \times \frac{h_c}{\phi_C}\right)^2 \frac{8\pi\rho\left(r_{pm} + \delta + t_y + {}^{h_c}/_2\right)}{\pi\phi_C^2}\,(\Omega) \tag{5}$$

$$I_\phi = \sqrt{\frac{P}{2R}} = \sqrt{\frac{150}{2R}} \tag{6}$$

where $W_c$ is the coil width in (m), $\xi$ the space factor equal to 0.6, $\phi_c$ the copper wire diameter in (m), $\rho$ the copper resistivity equal to $1.67 \times 10^{-6}\,\Omega \cdot \mathrm{m}$, $l$ the copper wire length in (m), $a$ the copper wire cross sectional area in ($\mathrm{m}^2$), $\delta$ the air gap length in (m), and $I_\phi$ the phase current in (A).

Based on the first stage of the design result, the permanent magnet radius $r_{pm}$ was identified by the addition of the height of the permanent magnet $h_{pm}$ with the shaft radius $r_s$. At this stage, the shaft radius $r_s$ is equal to 1 mm. During the second stage of design within the fixed radius of the permanent magnet $r_{pm}$, the shaft radius $r_s$ and height of the permanent magnet $h_{pm}$ were varied. The aim of the second stage of design is to strengthen the mover structure with an insignificant thrust reduction. The design flow of the PMLM is shown in Figure 4.

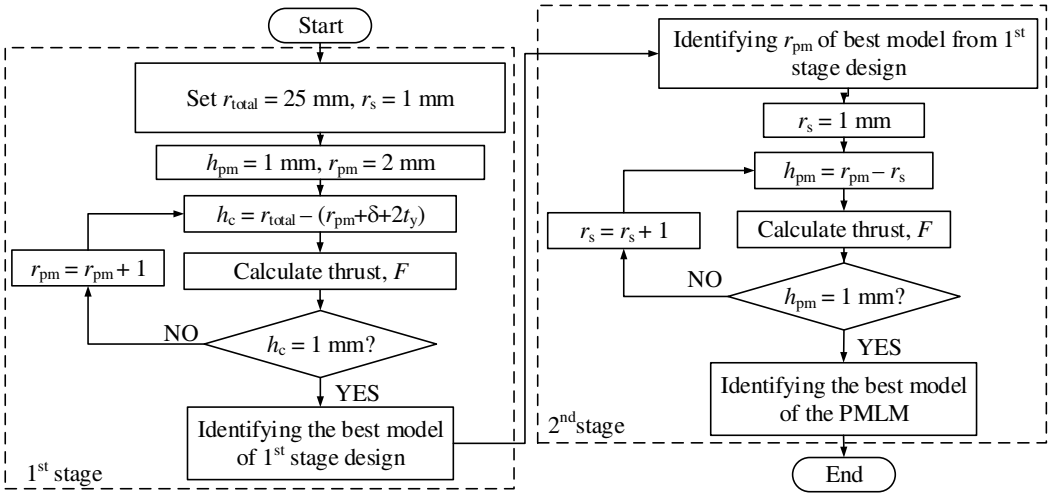


**Figure 4.** Design flow.

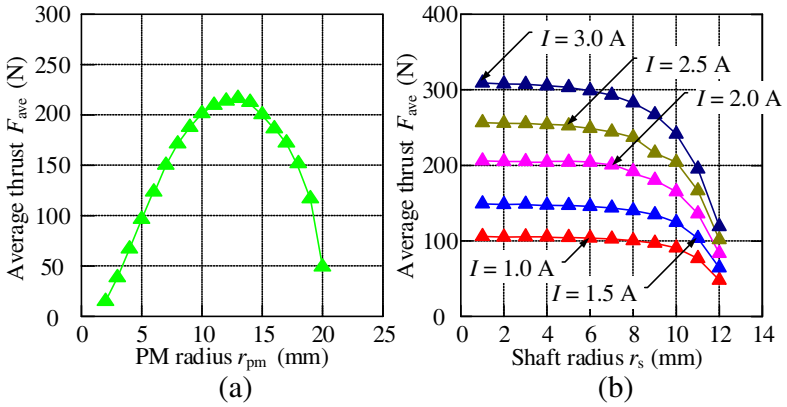


**Figure 5.** Result of PMLM design. (a) 1st stage. (b) 2nd stage.

Figure 5 shows the effects of the permanent magnet and shaft radii, $r_{pm}$ and $r_s$, to the average thrust $F_{ave}$ of the PMLM. Based on Figure 5(a), by increasing the permanent magnet radius $r_{pm}$, the average thrust $F_{ave}$ will also increase until it reaches the maximum value. This is due to the higher magnetic energy provided by the permanent magnet to produce a higher thrust. However, beyond the maximum point, the increment of the permanent magnet's size did not contribute to producing a higher thrust. Instead, the thrust is reduced despite the larger size of the permanent magnet. This is because a smaller-sized coil produces a lower magnetomotive force by the PMLM. Therefore, based on Figure 5(a), it is shown that the PMLM with an outer radius of the PM, $r_{pm}$, of 13 mm and the height of the coil, $h_c$, is 7.5 mm, which was selected as the best model for the first stage of design. For this model, the PMLM produced about 214 N of average thrust $F_{ave}$ at an input power $P$ of 150 W for each phase. At 150 W of input power, $P$, the current of the PMLM for each phase is equivalent to about 2.2 A. The effects of the shaft radius $r_s$ to the average thrust $F_{ave}$ of the PMLM are as shown in Figure 5(b). By increasing the shaft radius $r_s$, the height of the permanent magnet $h_{pm}$ was reduced. The reduction of the height of the permanent magnet $h_{pm}$ resulted in a reduction of the magnetic flux produced by the permanent magnet, hence the thrust $F$ decreased. Nevertheless, as shown in Figure 5(b), thrust reduction was not significant for a shaft radius $r_s$ below 6 mm, as opposed to when the shaft radius $r_s$ was higher than 6 mm. Therefore, the shaft radius $r_s$ of 6 mm was considered as optimal.

Based on the results of the second stage of design, the performance index of the PMLM was calculated. The performance index comparison between the designed PMLM with the commercialized

PMLM is as shown in Figure 6. The comparison was done with the volume $v$ of each linear motor model made as a reference. Based on Figure 6, it is shown that the designed PMLM is capable to produce a higher performance index than a similar volume $v$ of the commercialized PMLM. As mentioned previously, the linear motor performance depends on the input power $P$. Therefore, by using the motor constant square density $G$, the input power $P$ of each model of PMLM including the designed PMLM was normalized as shown in Figure 6(d). Figure 6(d) shows the capability of the designed PMLM to produce a higher thrust $F$ at a similar input power $P$ than a similar volume $v$ of the commercialized PMLM. On top of that, the performance index of the designed PMLM was above the limit line of the performance index of the commercialized PMLM.

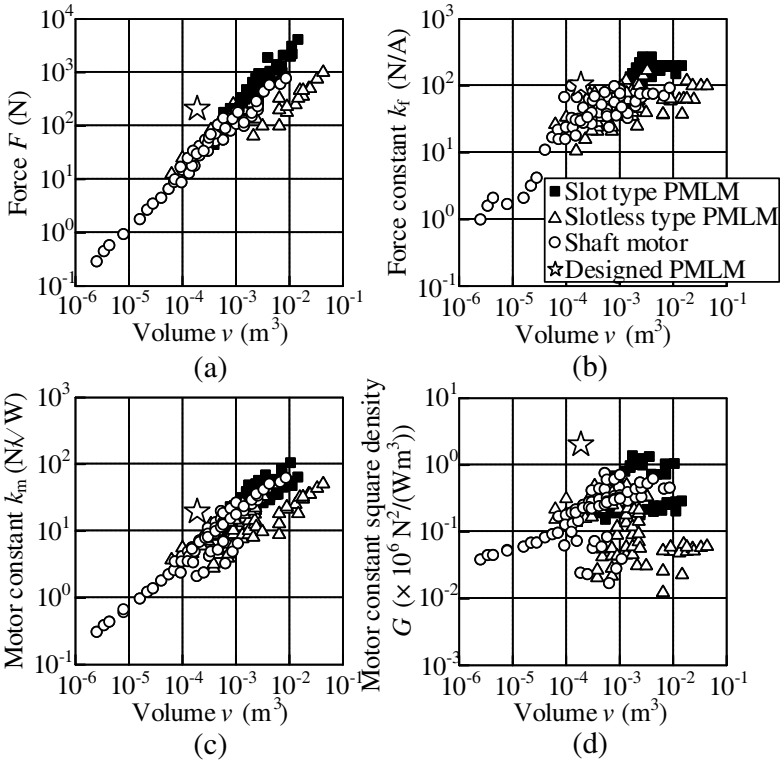


**Figure 6.** Comparison of performance index between designed PMLM with the commercialize PMLM. (a) Thrust, $F$. (b) Force constant, $k_f$. (c) Motor constant, $k_m$. (d) Motor constant square density, $G$.

## 4. STATIC THRUST CHARACTERISTICS MEASUREMENT OF THE PMLM

Based on the results of the design, the PMLM was manufactured. Figure 7 shows the manufactured PMLM. Since the driving system of the PMLM is still in the designing process, only a static thrust characteristic measurement was able to be conducted for the result validation. Figure 8 shows the experiment setup of the static thrust characteristic measurement.

The static thrust characteristics of the PMLM were measured for each individual phase and at a full scale of the mover displacement. Then, the measurement results of the static thrust characteristics were compared to a simulation output for a result validation. The static thrust characteristics of the PMLM at the current, $I = 1.5$ A, is as shown in Figure 9. Based on Figure 9, it is shown that the profile of the measured and simulated thrusts had a good agreement. However, a different maximum value was obtained between the measurement and simulation results. The profile of the thrust characteristics of the U and W phases were similar but inversed compared to each other. This is due to similar location of the coil but the inverse direction of the magnetic flux flow for both phases. This explained the similarity of the profile but an inverse in the direction. On the other hand, the profile of the V phase

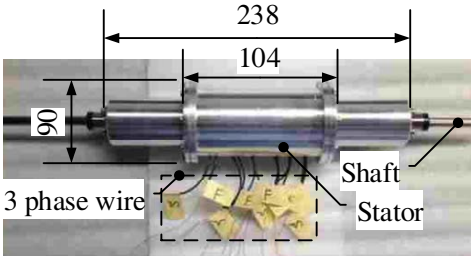


**Figure 7.** Assembled of the manufactured PMLM (unit: mm).

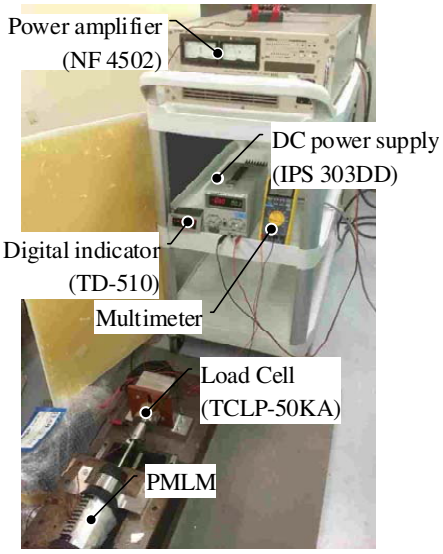


**Figure 8.** Experiment setup for static thrust characteristics measurement for the PMLM.

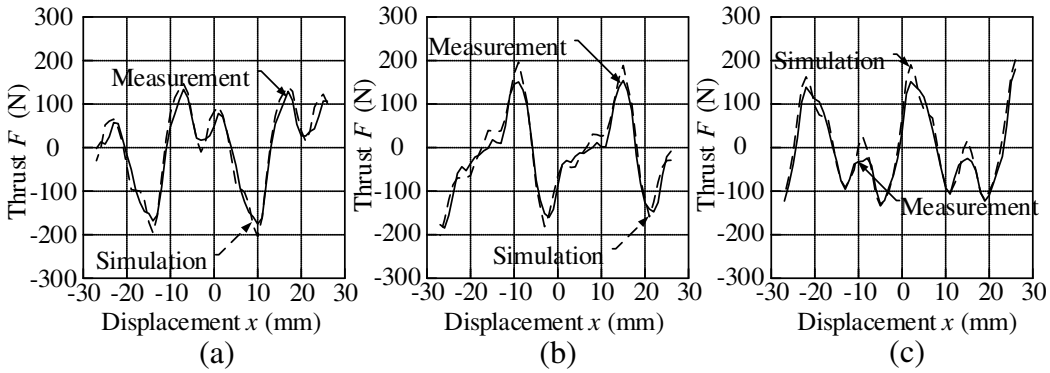


**Figure 9.** Static thrust characteristics of the PMLM for each phase and $I = 1.5$ A. (a) U phase. (b) V phase. (c) W phase.

thrust characteristics was different compared to the U and W phases. This is because the location of the V phase coil is in between the U and W phases.

## 5. CONCLUSIONS

The design of cylindrical permanent magnet linear motor (PMLM) has been discussed. The aim of the research is to design a high performance PMLM within fixed total radius $r_{total}$. The PMLM has undergone two stages of design. Several structure parameters have been varied. As a result, a PMLM that produces about 214 N at phase input power of 150 W has been designed. In order to prove its high performance characteristics, the designed PMLM performance has been compared to commercialized PMLM using four performance index. Based on the comparison, it is found that the PMLM has a capability to perform better than the commercialized PMLM with similar volume. On top of that, the designed PMLM also has performance index beyond the limitation of performance index of the commercialize PMLM. It can be seen especially on motor constant square density $G$ where the designed PMLM produced about $2.03 \times 10^6$ N$^2$/Wm$^3$. The PMLM was then manufactured, and the static thrust characteristics has been measured and compared to the simulation output. Based on the comparison, it is shown that the result of the measurement and simulation output had a good agreement.

## REFERENCES


1. Gieras, J. F. and Z. J. Piech, *Linear Synchronous Motors: Transportation and Automation Systems*, CRC, Boca Raton, FL, 2000.
2. Boldea, A. and S. Nasar, *Linear Electromagnetic Devices*, Taylor & Francis, New York, 2001.
3. Cao, R., M. Cheng, W. Hua, W. Zhao, and X. Sun, "Comparative study of linear double salient permanent magnet motors," *14th Biennial IEEE Conference on Electromagnetic Field Computation (CEFC)*, 1, 2010.
4. Dorrell, D. G., "Are wound-rotor synchronous motors suitable for use in high efficiency torque-dense automotive drive?," *38th Annual Conference on IEEE Industrial Electronics Society*, 4880–4885, 2012.
5. Norhisam, M., H. Ezril, F. Azhar, R. N. Firdaus, H. Wakiwaka, and M. Nirei, "Positioning system for sensor less linear DC motor," *Journal of the Japan Society of Applied Electromagnetics and Mechanics (JSAEM)*, Vol. 19, S91–S94, Supplement, 2011.
6. Yamamoto, Y. and H. Yamada, "Analysis of magnetic circuit and starting characteristics of flat-type linear pulse motor with permanent magnets," *T. IEE Japan*, Vol. 104-B, No. 5, 265–272, 1984.
7. Laithwaite, E. R., "Linear electric machines — A personal view," *Proceedings of the IEEE*, Vol. 63, No. 2, 250–290, 1975.
8. De Groot, D. J. and C. J. Heuvelman, "Tubular linear induction motor for use as a servo actuator," *Electric Power Applications, IEE Proceedings B*, Vol. 137, No. 4, 273–280, 1990.
9. Sanada, M., Y. Takeda, and T. Hiras, "Cylindrical linear pulse motor with laminated ring teeth," *Proceedings of the Second International Conference on Electronic Materials (ICEM'90)*, Vol. 2, 693–698, 1990.
10. Eastham, J. F., R. Akmese, and H. C. Lai, "Optimum design of brushless tubular linear machines," *IEEE Transactions on Magnetics*, Vol. 26, No. 5, 2547–2549, 1990.
11. Wang, J., G. W. Jewell, and D. Howe, "Design optimisation and comparison of tubular permanent machine topologies," *IEE Proceeding Electrical Power Applications*, Vol. 148, No. 5, 456–464, 2001.
12. Azhar, F., M. Norhisam, H. Wakiwaka, K. Tashiro, and M. Nirei, "Design and static characteristics of permanent magnet linear motor for oil palm cutter," *The 23th MAGDA Conference*, 389–394, 2014.
13. Masanobu, K., H. Toshiyuki, S. Toru, and O. Motomichi, "Development of high-force-density iron-core linear synchronous motor," *IEE J. Transactions on Industry Applications*, Vol. 132, No. 4, 480–486, 2012.
14. Nakaiwa, K., H. Wakiwaka, and K. Tashiro, "Study and consideration on thrust and harmonic distortion of small cylinder linear synchronous motor," *Journal of the Japan Society of Applied Electromagnetics and Mechanics*, Vol. 22, No. 2, 238–242, 2014.
15. Zare, M. R., M. Norhisam, C. V. Aravind, N. Mariun, I. Aris, and H. Wakiwaka, "Optimization of mover parameters in high thrust density transverse flux linear motor by genetic algorithm," *International Review of Electrical Engineering*, Vol. 7, No. 2, 3779–3786, 2012.
16. Firdaus, R. N., M. Norhisam, C. V. Aravind, M. Nirei, and H. Wakiwaka, "Improvement of energy density in single stator interior permanent magnet using double stator topology," *Mathematical Problems in Engineering*, 1–13, 2014.
17. Tavana, N. R. and V. Dinavahi, "Design of slotted permanent magnet linear synchronous motor for improved thrust density," *IEEE International Conference on Electric Machines & Drives (IEMDC)*, 1225–1228, 2013.
18. Li, L., Y. Tang, B. Kou, and M. Ma, "Design and analysis of ironless linear electromagnetic launcher with high thrust density for space platform," *16th International Symposium on Electromagnetic Launch Technology (EML)*, 1–6, 2012.
19. Mikami, T. and Y. Fujimoto, "Design of a high-thrust density spiral motor using finite element analysis," *38th Annual Conference on IEEE Industrial Electronics Society*, 5416–5421, 2012.